Electronic Supplementary Material (ESI) for Journal of Materials Chemistry A.

3D Urchin-shaped $Ni_3(VO_4)_2$ hollow nanospheres for high-performance asymmetric supercapacitor applications

Rudra Kumar, Prabhakar Rai*, Asutosh Sharma*

Department of Chemical Engineering, Indian Institute of Technology Kanpur, Kanpur 208016, India

*Email: prkrai@iitk.ac.in, ashutos@iitk.ac.in

Figure S1. XRD pattern of $Ni_3(VO_4)_2$ precursors synthesized by hydrothermal method.

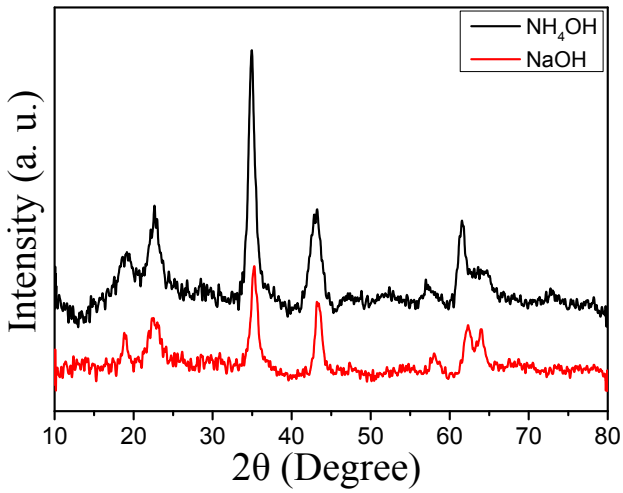

Figure S2. TGA-DTA curves of $Ni_3(VO_4)_2$ precursors synthesized by hydrothermal method using (a) NH_4OH and (b) NaOH.

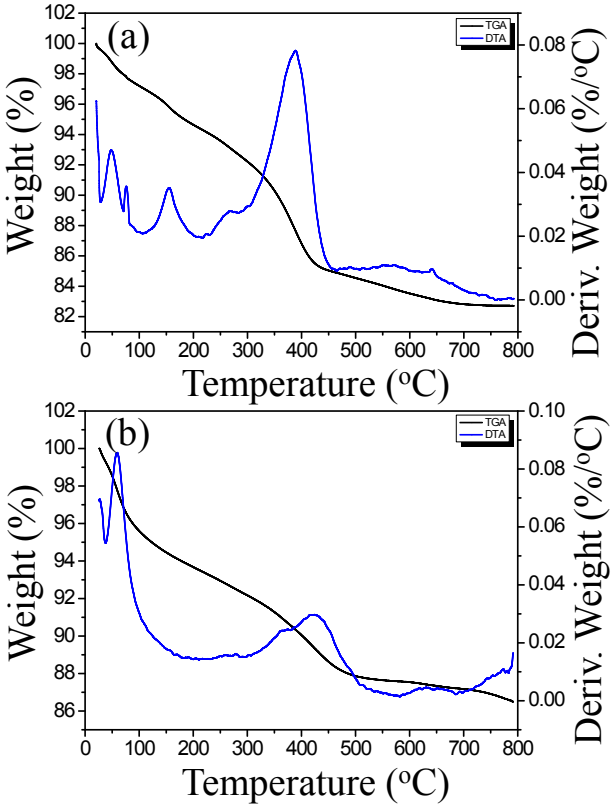

Figure S3. SEM images of $Ni_3(VO_4)_2$ nanostructures after hydrothermal synthesis; (a) nanospheres and (b) nanoparticles at 180°C for 20 h, (c) nanospheres at 180°C for 10 h and (d) nanospheres at 120 °C for 20 h.

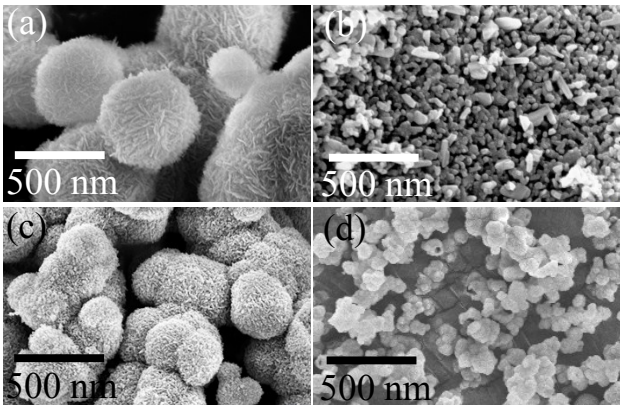

Figure S4. EDS analysis and elemental mapping of $Ni_3(VO_4)_2$ nanospheres.

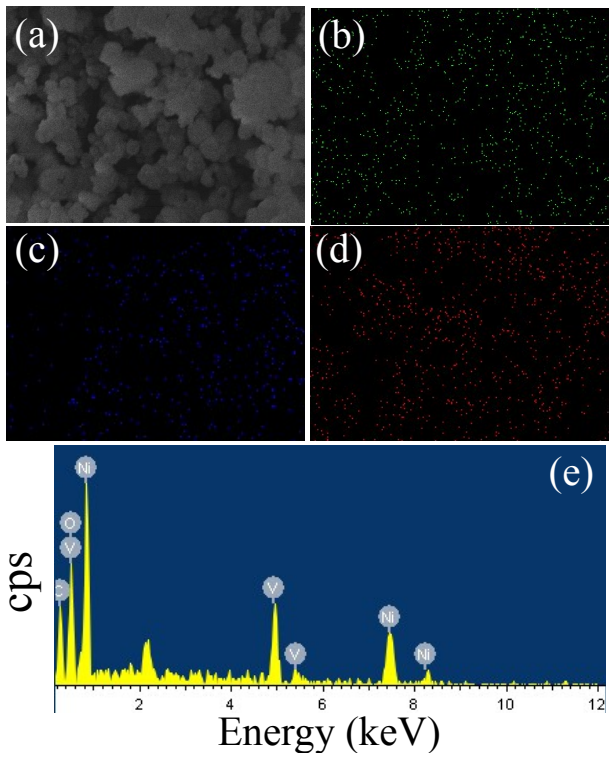

Figure S5. EDS analysis and elemental mapping of $Ni_3(VO_4)_2$ nanoparticles.

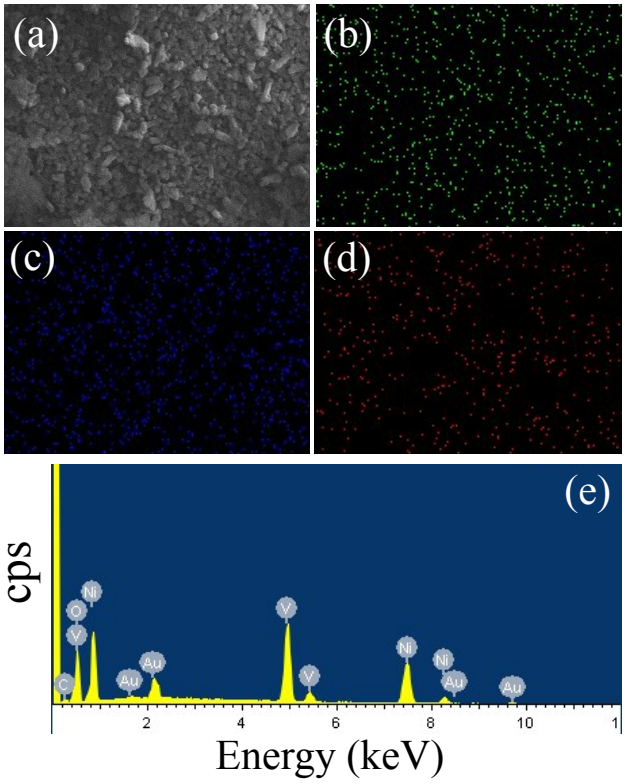

Figure S6. BET surface area and pore size distribution of $Ni_3(VO_4)_2$ nanostructures; (a) nanospheres and (b) nanoparticles.

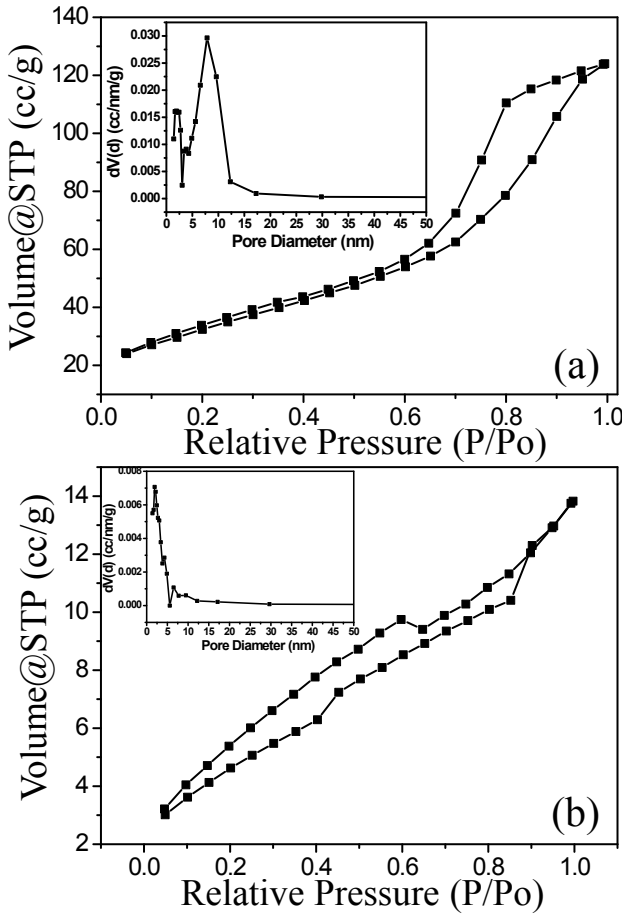

Figure S7. Photograph showing the change in colour of (a) $NiCl_2 \cdot 6H_2O$ solution after (b) NH_4OH and (c) NaOH addition.

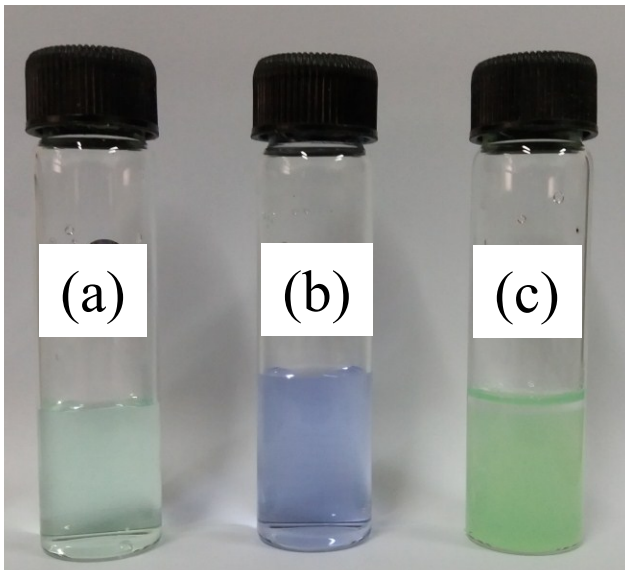

Figure S8. (a) UV-visible and (b) FTIR spectra of reaction intermediates formed during the synthesis of $Ni_3(VO_4)_2$ nanostructures.

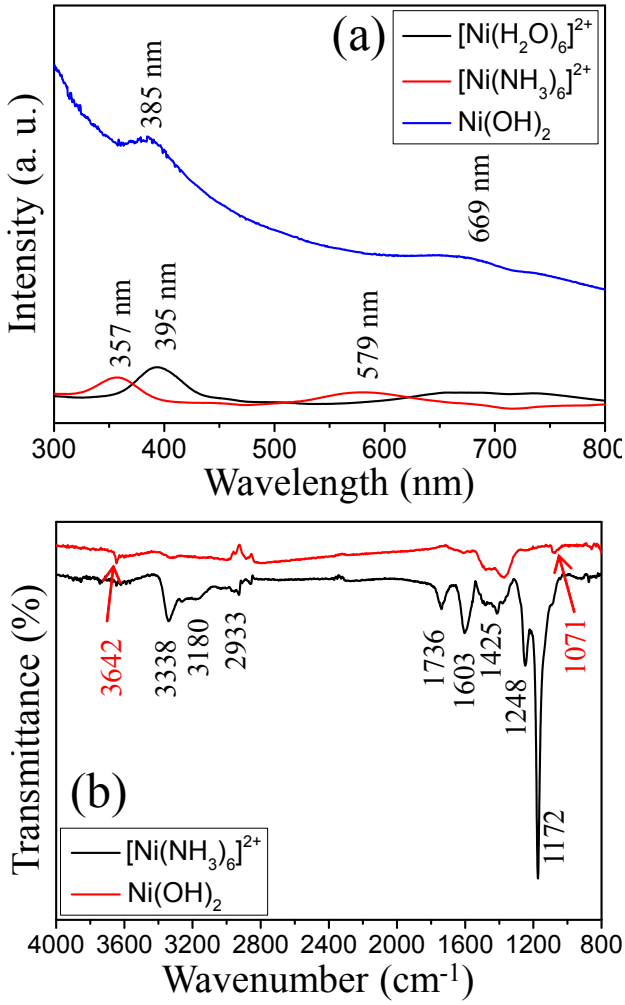

The formation of reaction intermediates has been confirmed by UV-visible and FTIR and spectroscopy. UV visible spectra of green $[Ni(H_2O)_6]^{2+}$ ions (hexaquonickel(II) ions) shows absorbance at 395 nm as shown in Fig. S8a.[1] The addition of NH_4OH resulted in blue shift in peak position from 395 to 357 due to the $[Ni(NH_3)_6]^{2+}{}_{(aq)}$ (hexamminenickel(II) ion) complex ions formation.[2] The origin of UV visible absorbance in these complexes is related to crystal field splitting of d orbital of nickel.[3] In an octahedral complex, the metal is at the centre of the octahedron and ligands are at the six corners. Thus under the influence of an octahedral ligand field the d orbitals split into two groups (e_g and t_{2g}) of different energies. The

difference in the energy between the two d levels is given by Δo or 10Dq. The two e_g (d_{x2-y2} and d_{z2}) orbitals are 6Dq above the average level and three t_{2g} (d_{xy}, d_{yz}, d_{xz}) orbitals are 4Dq below the average. The magnitude of crystal field splitting depends on the nature of ligand. Since, NH_3 is stronger ligand than H_2O, hence it cause larger crystal field splitting and therefore absorption peak was blue-shifted. The formation of $Ni(OH)_2$ in NaOH medium was confirmed from absorption peak at 385 nm.[4]

The formation of these intermediates has also been confirmed by FTIR spectra and shown in Fig. S8b. In $Ni(OH)_2$, the band at 3642 cm^{-1} and a strong absorption at 1400-1600 cm^{-1} can be ascribed to the stretching and bending modes of surface-adsorbed/trapped (hydrogen-bonded) water molecules, indicating the presence of water molecules in the structure. Ni−OH bending vibrations result in typical absorption bands at low wavenumbers, such as at 1071 cm^{-1}, in agreement with the previous reports.[5] In $[Ni(NH_3)_6]^{2+}$ complex ions, NH_3 asymmetric and symmetric stretching vibrations were found at 3338 and 3180 cm^{-1}, respectively. In the bending region, the band at 1603 and 1172 cm^{-1} was due to asymmetric and symmetric H- N-H deformation, respectively.[6] The prominent bands at 2850–2950 are typical of C–H symmetric stretching and bending vibrations, respectively. This confirms incomplete removal of ethanol.[7] Thus, UV-visible and FTIR spectra confirmed the formation of two kinds of intermediates during $Ni_3(VO_4)_2$ nanostructures synthesis, which guided the growth process and resulted in the formation of different morphologies.

Figure S9. (a) CV and (b) GCD curve of $Ni_3(VO_4)_2$ nanoparticles.

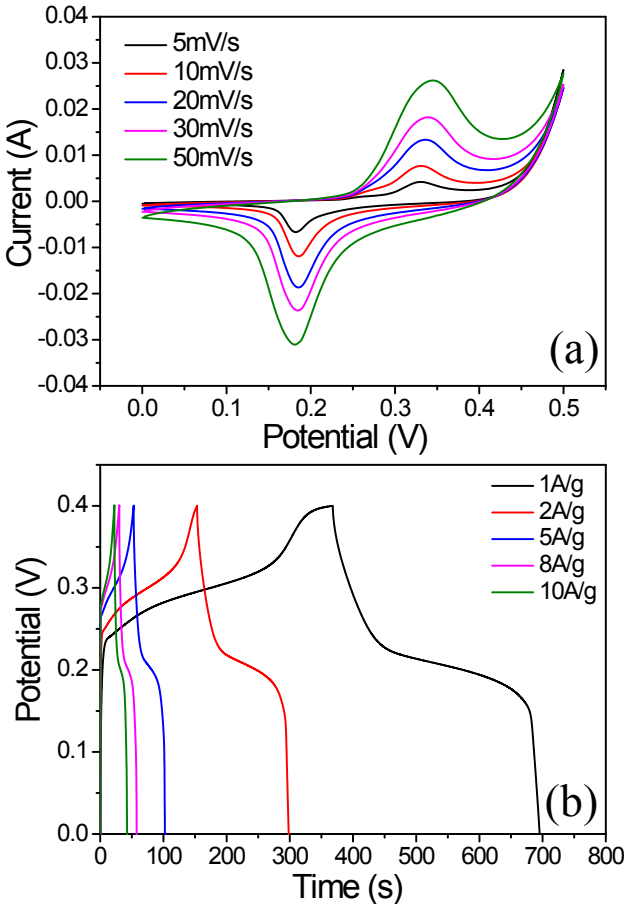

Figure S10. (a) Rate capability and (b) long term stability of $Ni_3(VO_4)_2$ nanospheres.

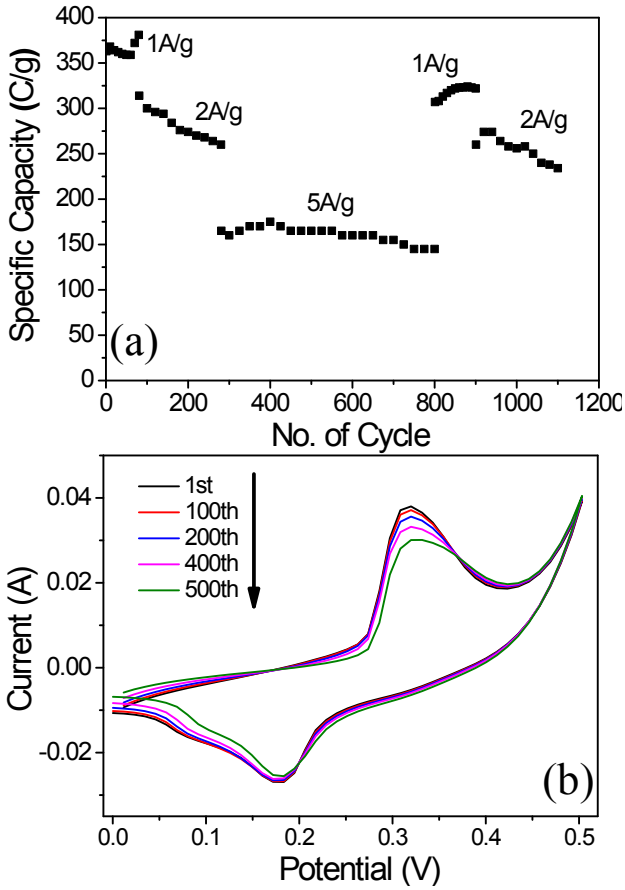

Figure S11. (a) CV and (b) GCD curve of bare Ni foam and $Ni_3(VO_4)_2$ nanospheres.

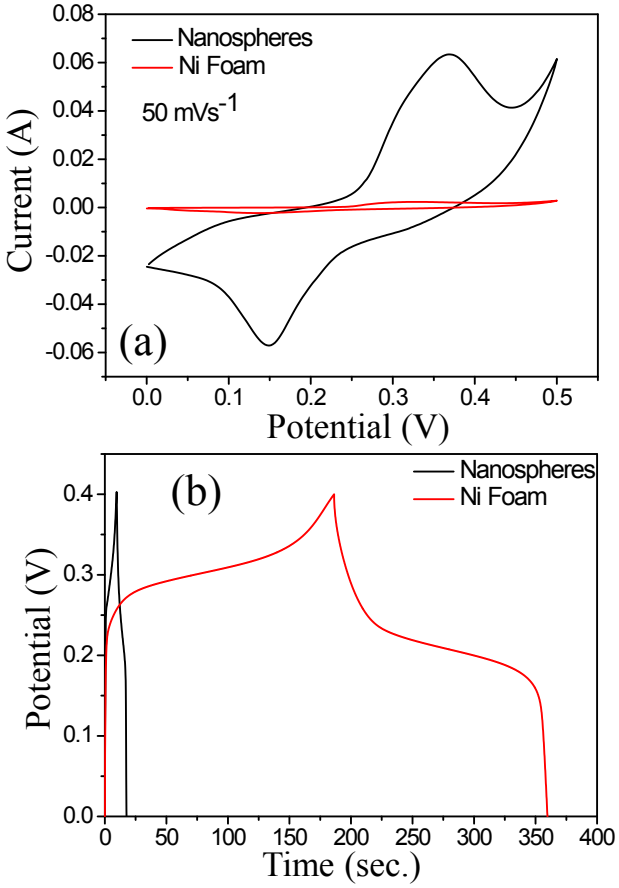

Table S1. Comparison of asymmetric supercapacitor performance of our electrodes with others full cell device reported in literature.

Asymmetric Supercapacitor	**Voltage (V)**	**Energy Density ($Whkg^{-1}$)**	**Power Density (Wkg^{-1})**	**Cyclic Stability**	**Ref. No**
AC//$Co(OH)_2$/Ni foam	1.6	20.3	90.6	69% (1000)	8
3D rGO//$Ni(OH)_2$	1.7	39.9	-	95% (3000)	9
AC//$Ni(OH)_2$@3D Ni	1.3	21.8	660	96% (3000)	10
AC//$Ni(OH)_2$/XC-72	1.6	36	490.7	85% (1000)	11
Ni_3S_2/MWCNT-NC//AC	1.6	19.8	798	90 %(5000)	12
AC//Co_3O_4NSs–rGO	1.5	13.4	2166	89% (1000)	13
VN//$Co(OH)_2$	1.6	22	160	82% (1000)	14
Ni/VN//$Ni_{1-x}V_xO_2$	1.6	23.3	176.7	87% (1000)	15

AC//$NiCo_2O_4$NSs@HMRAs	1.5	15.42	-	106% (2500)	16
AC//CuO	1.4	19.7	700	96% (3000)	17
$Ni_3(VO_4)_2$//AC	1.6	25.3	240	92% (1000)	This work

References;

1. G. M. Wieder, *J. Chem. Edu.*, 1986, **63**, 988-989.
2. C. K. Jørgensen, *Acta Chem. Scand.*, 1956, **10**, 887-910.
3. D. F. Shriver and P. W. Atkins, *Inorganic Chemistry*, Oxford University Press, 3rd edition, 2001, 227-236.
4. Y. Qi, H. Qi, J. Li and C. Lu, *J. Cryst. Growth*, 2008, **310**, 4221– 4225.
5. D. S. Hall, D. J. Lockwood, S. Poirier, C. Bock and B. R. MacDougall, *J. Phys. Chem. A*, 2012, **116**, 6771−6784.
6. E. Mikuli, A. Migdał-Mikuli and D. Majda, *J. Therm. Anal. Calorim.*, 2013, **112**, 1191–1198.
7. W. Xing, F. Li, Z.-F. Yan and G. Q. Lu, *J. Power Sources*, 2004, **134**, 324–330.
8. S. Yang, K. Cheng, K. Ye, Y. J. Li, J. Qu, J. L. Yin, G. L. Wang and D. X. Cao, *J. Electroanal. Chem.*, 2015, **741**, 93–99.
9. F. Luan, G. M. Wang, Y. C. Ling, X. H. Lu, H. Y. Wang, Y. X. Liu and Y. Li, *Nanoscale*, 2013, **5**, 7984–7990.

10. Y. Z. Su, K. Xiao, N. Li, Z. Q. Liu and S. Z. Qiao, *J. Mater. Chem. A*, 2014, **2**, 13845–13853.
11. L. Sui, S. Tang, Z. Dai, Z. Zhu, H. Huangfu, X. Qin, Y. Deng and G. M. Haarberg, *New J. Chem.*, 2015, **39**, 9363-9371.
12. C. S. Dai, P. Y. Chien, J. Y. Lin, S. W. Chou, W. K. Wu, P. H. Li, K. Y. Wu and T. W. Lin, *ACS Appl. Mater. Interfaces*, 2013, **5**, 12168.
13. C. Yuan, L. Zhang, L. Hou, G. Pang and W. C. Oh, *RSC Adv.*, 2014, **4**, 14408–14413.
14. R. Wang, X. Yan, J. Lang, Z. Zheng and P. Zhang, *J. Mater. Chem.* A, 2014, **2**, 12724–12732.
15. C. Ji, J. Bi, S. Wang, X. Zhang and S. Yang, *J. Mater. Chem. A*, 2016, **4**, 2158-2168.
16. X. F. Lu, D. J. Wu, R. Z. Li, Q. Li, S. H. Ye, Y. X. Tong and G. R. Li, *J. Mater. Chem. A*, 2014, **2**, 4706–4713.
17. S. E. Moosavifard, M. F. El-Kady, M. S. Rahmanifar, R. B. Kaner and M. F. Mousavi, *ACS Appl. Mater. Interfaces*, 2015, **7**, 4851–4860.